THE JOURNAL OF PHYSICAL CHEMISTRY B

Article

pubs.acs.org/JPCB

QM/MM Study on the Catalytic Mechanism of Heme-Containing Aliphatic Aldoxime Dehydratase

Xiao-Liang Pan, Feng-Chao Cui, Wei Liu, and Jing-Yao Liu*

State Key Laboratory of Theoretical and Computational Chemistry, Institute of Theoretical Chemistry, Jilin University, Changchun 130023, China

ABSTRACT: Aliphatic aldoxime dehydratase (Oxd) catalyzes the dehydration of aliphatic aldoximes (R−CH═N−OH) to the corresponding nitriles (R−C≡N). Quantum mechanics/molecular mechanics (QM/MM) calculations are performed to elucidate the catalytic mechanism of the enzyme on the basis of the X-ray crystal structure of the Michaelis complex. On the basis of the calculations, we propose a complete catalytic cycle of Oxd in which the distal histidine (His320) acts as a general acid/base. In the Michaelis complex, the elimination of the hydroxyl group of aldoxime is facilitated by His320 donating a proton to the hydroxyl group in a concerted way, which is the rate-limiting step. The formed intermediate has a ferric heme iron and an unpaired electron on the nitrogen atom of the substrate coupled to a singlet state. The second step is the deprotonation of the β-hydrogen of the substrate by His320 after the substrate rotates about the Fe−N bond for ∼180° to yield the neutral product. In the meantime, the heme iron goes back to ferrous state by a one-electron transfer from the substrate to the ferric heme iron, and His320 goes back to the protonated state to proceed with the following reaction. The functions of the protein environment and the active site residues are also discussed.

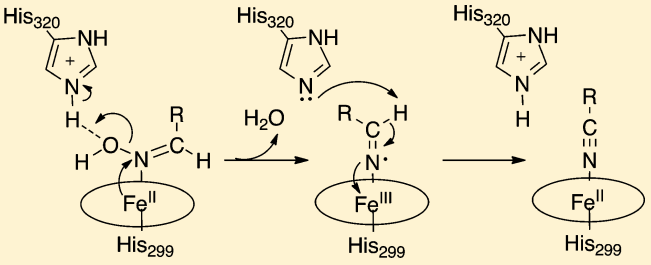

INTRODUCTION

Aliphatic aldoxime dehydratase (Oxd) is a newly discovered heme-containing enzyme (EC 4.99.1.5) that catalyzes the dehydration of aliphatic aldoximes to the corresponding nitriles (Scheme 1). Due to the potential application for the production of nitriles under mild conditions and the unique characters of the reaction mechanism, Oxd reaction has been the subject of extensive experimental studies. Oinuma et al. first purified and characterized the enzyme from *Pseudomonas chlororaphis* B23 (OxdA) and identified it as a hemoprotein. They also found that the enzyme reaction proceeded when the heme iron of Oxd was in the ferrous state, and these aldoxime dehydration reactions would involve the direct approach of the substrate to the heme iron.[1] Later Oxds from other origins had been purified and characterized (OxdRG from *Rhodococcus globerulus* A-4,[2] OxdRE from *Rhodococcus* sp. N-771,[3] and OxdK from *Pseudomonas* sp. K-9[4]). Oinuma et al. characterized the heme environment in OxdA using resonance Raman spectroscopy and demonstrated that the OxdA heme contained a proximal histidine ligand.[5] Konishi et al. identified two crucial histidines, namely, His299 and His320, using site-directed mutagenesis and spectroscopic analysis, and proposed the Oxd reaction mechanism for the first time.[6] Later, two reaction intermediates (namely, OS-I and OS-II, following the notations of the original papers) were discovered and characterized.[7,8] The first one is actually the Michaelis complex in which the substrate binds to the ferrous heme iron via its nitrogen atom forming a six-coordinate low-spin heme.[7] The second one is the reaction intermediate after the dehydration step and is proposed to include a highly oxidized heme with strong bonding between the substrate and the heme iron.[8] It has been reported that the dehydration of aldoximes can be catalyzed by some cytochrome P450 that shared no sequence similarity with the aldoxime dehydratase family,[9] and a similar intermediate with ferryl state heme iron has been suggested in the proposed catalytic mechanisms.[10,11]

Scheme 1. Reaction Catalyzed by Oxd

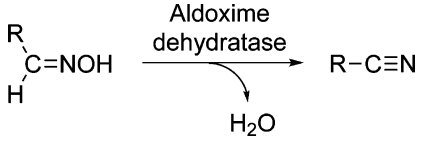

Recently, by reduction of a substrate-bound ferric Oxd complex using X-ray radiation under cryogenic temperature, the X-ray crystal structure of the Michaelis complex of OxdRE has been determined at 1.6 Å resolution,[12] which provides an opportunity to explore the catalytic mechanism through theoretical calculations. The active site structure of the Michaelis complex is consistent with the previous proposed mechanism, and highlights some important residues for the reaction. Although the Oxd reaction has been through extensive experimental studies, some detailed aspects of the reaction mechanism are still unclear, for example, the electronic

Received: March 4, 2012
Revised: April 26, 2012
Published: May 3, 2012

dx.doi.org/10.1021/jp302114d | J. Phys. Chem. B 2012, 116, 5689−5693

structures of the species along the catalytic cycle. Especially, the electronic structure of the second intermediate OS-II, which has been proposed to have a ferryl heme iron and an Fe=N double bond, is not only theoretically intriguing, but also may be the key to understanding the reaction mechanism. Additionally, although the β-hydrogen of the substrate has been proposed to be able to be deprotonated by a weak base in the active site,[8] no such residue or solvent molecule has yet been proposed.

The combined quantum mechanics and molecular mechanics (QM/MM) method has become the standard tool for modeling heme proteins in recent years. The basic idea is to describe the active site by QM, e.g., density functional theory (DFT), while to account for the effect of protein environment by MM.[13,14] In this study, we have used the QM(DFT)/MM method to investigate the reaction mechanism of Oxd, and tried to solve the above-mentioned issues and propose a complete catalytic cycle (Scheme 2).

Scheme 2. Suggested Catalytic Cycle for Oxd Based on the Present Calculations

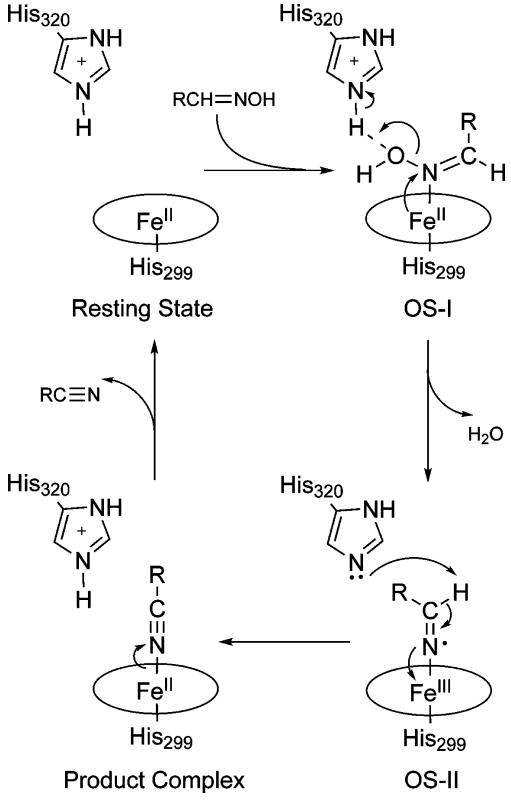

METHODS

To prepare suitable initial structures for the QM/MM calculations, we started from the X-ray crystal structure of the Michaelis complex of aldoxime dehydratase and propionaldoxime at 1.6 Å resolution (PDB code 3A16), and built a complete model of the solvated enzyme by adding missing hydrogen atoms and solvating the enzyme into a water sphere of 25 Å radius centered on the heme iron. No counterions were introduced to neutralize the system. The complete system consists of 9866 atoms, including 4317 atoms in the solvent. The system then was relaxed by performing pure force field energy minimizations and molecular dynamics (MD) simulations, using the CHARMM22 force field[15] as implemented in the CHARMM program,[16] during which stochastic boundary conditions[17,18] were imposed to keep the solvent water from running into vacuum. The coordinates of the entire heme unit and the coordinating His299 and propionaldoxime were kept fixed during the MD simulations because the CHARMM force field parameters for the substrate and the heme are of relatively poor quality due to the lack of extensive validation of the parameters for the substrate and the insufficiency of the molecular mechanics force fields to treat the transition metal complexes.

The QM/MM calculations started from the geometry of a representative snapshot in the equilibrated ensemble and concerned a QM region with 109 QM atoms (including the side chains of residues Glu143, Arg178, Ser219, His299, and His320, heme without the side chains, the substrate, and 13 hydrogen linked atoms). In the QM/MM geometry optimizations, the QM region and 2077 MM atoms (defined by including all residues within 15 Å of the heme iron) were allowed to relax, whereas the remaining MM atoms were frozen. The QM method employed in the present calculations is the spin-unrestricted B3LYP hybrid density functional. The iron atom is described by the LANL2DZ basis set, while 6-31G(d) is used for all other atoms. Single point calculations with a larger basis set (6-311++G(d,p)/LANL2DZ) were performed on the optimized geometries. An electronic embedding scheme[19] was applied, and the QM/MM electrostatic interactions were evaluated from the QM electrostatic potential and the MM atomic charges. No cutoffs were introduced for the nonbonding MM and QM/MM interactions. To treat the QM/MM boundary, we used hydrogen link atoms with the charge shift model.[20] The QM program employed in the QM/MM was TURBOMOLE.[21] All QM/MM calculations were performed with the ChemShell package.[22,23] The CHARMM22 force field run through the DL-POLY program[24] was used for the treatment of the MM part of the system. Geometry minimizations were done with the DL-FIND optimizer[25] of ChemShell in hybrid delocalized internal coordinates (HDLC)[26] applying the default convergence criteria. Nudged elastic band (NEB)[27] and dimer methods[28] are used to locate the transition state structure.

RESULTS AND DISCUSSION

Dehydration Step. The calculations started from the X-ray crystal structure of the Michaelis complex. Unlike most of the heme proteins, Oxd binds the substrate to the heme iron directly in the Michaelis complex. It has been found that the OS-I (Michaelis complex) is in a low-spin ferrous state based on resonance Raman data,[7] suggesting that Fe^{II}Por, in a singlet state, binds aldoxime in a coordinative dative bond, involving the lone pair on N and the empty d_{z^2} orbital of the ferrous iron. The DFT(B3LYP)/MM calculations for OS-I yield a ground state with closed-shell singlet state configuration, consistent with the experimental observations. The optimized structure of OS-I replicates the crystal structure very well (Figure 1a). Natural population analysis (NPA) was applied to the optimized structures of the enzyme–substrate complex, the His–heme–substrate complex, and the gas-phase substrate (Table 1). Comparing the natural charges of the substrate in the gas phase and in the His–heme–substrate complex, there is a lower electron density on the leaving hydroxyl group and C=N moiety due to the charge transfer from the substrate to the heme iron. In the protein environment, the electron density on

dx.doi.org/10.1021/jp302114d | J. Phys. Chem. B 2012, 116, 5689–5693

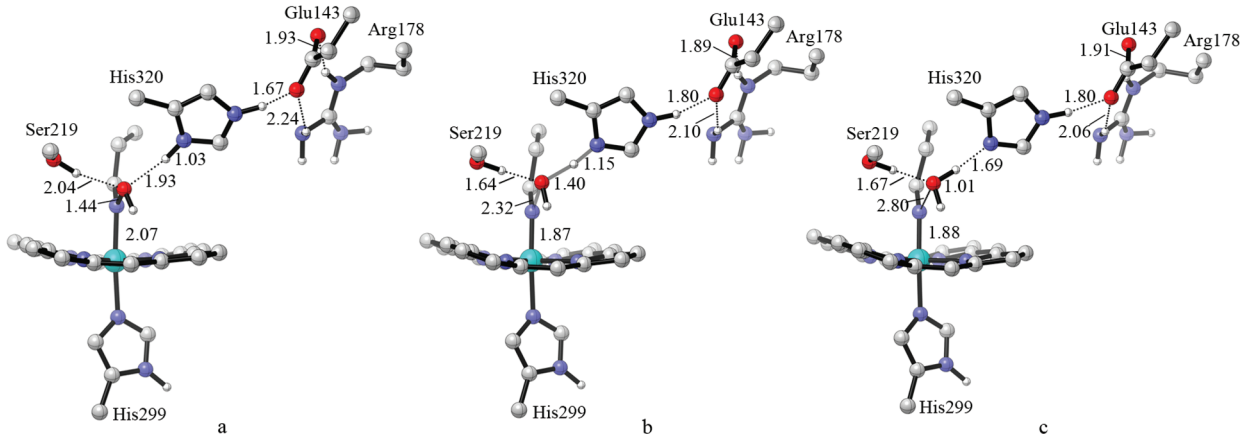

Figure 1. QM atoms of the optimized structures of (a) the Michaelis complex (OS-I), (b) the transition state structure (TS-I), and (c) the intermediate (Int) for the dehydration step. Hydrogen atoms in C−H bonds are hidden for clarity. Distances are given in angstroms (Å).

Table 1. Natural Charges of the Substrate with Hydrogens Summed into Heavy Atoms

heavy atom	enzyme−substrate	his−heme−substrate	gas phase
O	−0.12	−0.05	−0.10
N	−0.13	−0.05	−0.15
C_α	0.42	0.33	0.25
C_β	−0.01	−0.01	−0.02
C_γ	0.04	0.02	0.02
sum	0.20	0.24	0.00

the leaving hydroxyl group is increased due to the enhancement of the polarization of the substrate, so the elimination of the hydroxyl group is facilitated.

The calculations show that the dissociation of hydroxide and the forming of water take place in a concerted step with an energy barrier of 16.6 (12.8) kcal/mol and are endothermic by 10.1 (4.7) kcal/mol at the B3LYP/[6-31G(d)/LANL2DZ]/MM level (Figure 1). Values in the parentheses are single point energies at the B3LYP/[6-311++G(d,p)/LANL2DZ]/MM level. Judging from the structure similarity and the endothermic, the transition state is a so-called late transition state. The Fe−N bond is shortened by 0.30 Å in TS-I and slightly longer in Int than TS-I, suggesting that the heme can bind the substrate more tightly in TS-I and Int than in OS-I. His320, which is assumed to be in the protonated state and acts as a general acid in this step, supplies the δ-hydrogen to facilitate the elimination of the hydroxyl group in a concerted way. The hydrogen bond between Glu143 and N_ε of His320 becomes weaker in the TS structure and hence destabilizes the TS structure, although this trend can be compensated by a stronger interaction between Glu143 and Arg178 in the TS structure. On the other hand, Ser219, which is hydrogen-bonded to the substrate in OS-I, forms a stronger hydrogen bond with the leaving hydroxyl group due to an accumulation of negative charge on the oxygen atom, and hence stabilizes the TS structure.

Following the notations of ref 8, the reaction intermediate formed after the departure of the water molecule is named OS-II (Figure 2a). OS-II was proposed to have a highly oxidized heme iron and an Fe═N double bond in the previous experimental work.[8] However, the DFT(B3LYP)/MM calculation shows that, during the reaction process, the closed-shell state reactant breaks the spin symmetry and turns into an open-shell singlet state. The spin density of OS-II mainly concentrated on iron (0.91) and nitrogen atom (0.79) and $\langle S^2 \rangle$ is 0.94, indicating there is a one-electron transfer from heme iron to the substrate during the reaction, and OS-II has a

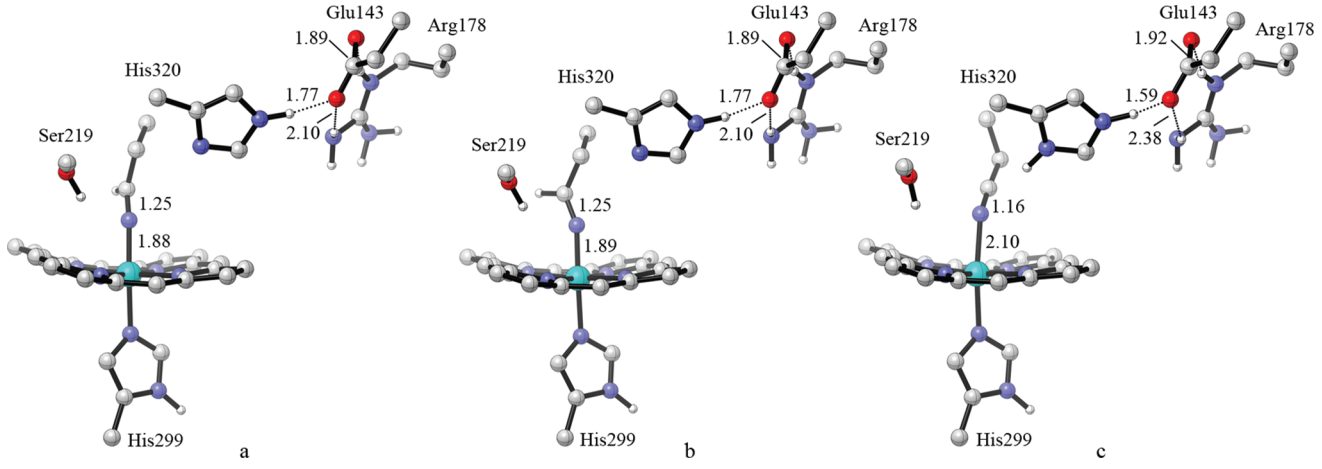

Figure 2. QM atoms of the optimized structures of (a) the intermediate (OS-II), (b) the transition state structure (TS-II, scanned), and (c) the product complex (PC) for the deprotonation step. Hydrogen atoms in C−H bonds except the transferring hydrogen are hidden for clarity. Distances are given in angstroms (Å).

dx.doi.org/10.1021/jp302114d | J. Phys. Chem. B 2012, 116, 5689−5693

diradical nature. When two unpaired electrons appear on closely neighboring atoms, there can exist a finite amount of electronic overlap between them. So the singlet state $Fe^{III}-N^{\bullet}$ can be seen as possessing a dative σ bond and a weakly coupled bond, similar to the bonding feature of oxy-ferrous in myoglobin[29] and P450.[30] As a result, the bonding between the heme iron and the substrate is stronger in OS-II, which is in accordance with the higher vibrational frequency corresponding to the Fe−N bond stretching observed in the resonance Raman spectroscopy.[8] However, this result does not support a ferryl heme intermediate, which will require a second electron transfer from heme iron to the substrate. Such a ferryl−anion complex would require a singlet ferryl heme iron which is not a low-lying electron configuration in order to maintain the total spin.

We also calculated the optimized structure of the intermediate in the gas phase, and although the ground state is still an open-shell singlet in the gas phase, the spin density is mainly concentrated on iron and porphyrin, so the electronic configuration can be seen as $Fe^{III}Por^{\bullet+}{=}N^{-}{=}CH-R$, which corresponds to the transfer of one more electron from the heme (porphyrin) to the substrate. However, this electronic configuration is unfavored in the protein environment, which is consistent with the experimental results,[8] and the configuration $Fe^{III}Por-N^{\bullet}{=}CH-R$ is stabilized and becomes the ground state in the protein environment .

Deprotonation Step. To yield the final nitrile product, the reaction intermediate OS-II needs to lose the hydrogen atom on the carbon bearing the nitrogen atom. It has been proposed that this hydrogen atom should be very acidic due to the intramolecular electron transfer from the substrate to the heme, and should be very easily removed by a near-by weak base in a fast step.[8] In the meantime, the ferrous heme should be regenerated, and His320 should be protonated again to proceed with the next catalytic cycle. However, the active site of Oxd is a hydrophobic pocket, and no candidate responsible for the deprotonation and/or protonation, such as polar residue or solvent molecule, has been proposed yet. On the basis of the above discussions, we propose the mechanism of the depronation of the β-hydrogen of the substrate as below. After the departure of the water molecule yielded during the dehydration step, the substrate rotates about the Fe−N bond for~180°, and the β-hydrogen of the substrate migrates to the ε position of His320 simultaneously to get the protonated His320, while one electron transfers from the substrate to the heme to recover the ferrous heme complexed with the neutral product.

This mechanism is supported by our calculations. Due to the diffusive nature of the rotation process, i.e., low barrier and relatively long reaction path, no true transition state structure was located. Instead, we did a relaxed scan of the dihedral $H_{\beta}-N_{\alpha}-Fe-N_{Por}$ to obtain an approximate energy profile about the rotation process. The highest point on the profile is 4.3 (3.9) kcal/mol higher in potential energy than OS-II (Figure 2). From any of the down hill points on the profile, an unconstrained optimization of the structure leads to the migration of the proton from the β position of the substrate to the ε position of His320 spontaneously, and the final product is 34.2 (37.2) kcal/mol lower in potential energy than OS-II. So we conclude that the deprotonation step consists of a low-barrier rotation process and a subsequent barrierless proton migration process.

The Fe−N bond is 0.22 Å longer in the product complex (PC) than in OS-II, and even slightly longer than in OS-I, indicating a weaker binding of the product than the reactant and the intermediate, which will be an advantage for the release of product. The formal bond order between N and C becomes three from two, which is reflected by a shorter bond in the product. For a perfect sp hybridization of triple-bonded C and N, the C, N, and Fe should be in a linear configuration, i.e., the angle C−N−Fe should be close to 180°. However, the angel C−N−Fe is 146.9° in PC, and the Fe−N bond is 0.13 Å longer than that in a gas-phase calculation, suggesting that such a product binding is unfavored in the active site, so the release of the product from the active site is facilitated. The hydrogen bond between Glu143 and His320 is strengthened in PC and helps to stabilize the protonated His320.

Comparing the energy barriers of the two steps, it can be concluded that the rate-limiting step is the dehydration step, and OS-II has a very short lifetime, consistent with the experimental observations.[7] Interestingly, Konishi et al. found that the deprotonation step would become the rate-limiting step on the addition of a large amount of aldoxime. They proposed that that a water molecule is attracted to the heme pocket of Oxd because of the accumulation of nitriles (and aldoximes), which are polar molecules, or that the water molecule yielded during the reaction from OS-I to OS-II could not reach an outer active site due to the accumulation of nitriles (and aldoximes), and this water molecule could protonate the weak base responsible for the deprotonation of the substrate.[8] However, it is hard for a weak base to extract a proton from a water molecule. Even if the water molecule protonated the weak base, the yielded OH^{-} could deprotonate the substrate afterward. Also, based on our proposed mechanism of the deprotonation step, the weak base is His320, and the deprotonation requires a rotation of the substrate, so the change of the rate-limiting step may be caused by the fact that the water molecule blocks the rotation of the substrate or the migration of the proton from the substrate to His320, and the alternative deprotonation pathways are far less efficient. To verify this speculation, we calculated the energy profile of the rotation process of the substrate starting from OS-II with the water molecule kept in the active site. The highest point on the profile is 0.5 kcal/mol higher in potential energy than the TS structure of the dehydration step. Due to the presence of the water molecule, the substrate did not have a direct contact with His320 after the rotation. So the β-hydrogen of the substrate could not migrant to the ε position of His320 simultaneously. Then we located the transition state structure of the concerted proton migration reaction between the substrate and His320 using the water molecule as a mediate, and the TS structure is 4.7 kcal/mol higher in potential energy than the TS structure of the dehydration step. So this result supports the speculation that the deprotonation step becomes the rate-limiting step when the water molecule yielded during the reaction from OS-I to OS-II does not leave the active site due to the addition of a large amount of aldoxime, and blocks the migration of the proton from the substrate to His320.

CONCLUSION

In this study, we used the QM(DFT)/MM method to investigate the catalytic mechanism of aliphatic aldoxime dehydratase. The results showed that the catalytic reaction proceeds on the singlet state surface. The catalytic residue His320 acts as a general acid in the dehydration step by

donating a proton to the leaving hydroxyl group of aldoxime in a concerted way, accompanied by a one-electron transfer from the ferrous heme iron to the substrate. The formed intermediate has a singlet diradical nature—a ferric heme iron and an unpaired electron on the neighboring nitrogen atom of the substrate—which forms an extra weakly coupled bond and thus a strong bonding between the heme iron and the substrate. After the water molecule formed in the dehydration step leaves the active site, the substrate in the intermediate rotates about the Fe−N bond for ∼180°, and again, the catalytic residue His320 acts as a general base by extracting the β-hydrogen of the substrate, accompanied by a one-electron transfer from the substrate to the ferric heme iron to yield the neutral product and the catalytically active ferrous heme iron. In the meantime, His320 becomes the protonated state to proceed with the following reaction. After the release of the product and the binding of another substrate, the catalytic cycle is completed.

The protein environment can enhance the polarization of the substrate to accumulate more negative charge on the oxygen atom of the leaving hydroxyl group, thus facilitating the dehydration step, and can stablize the open-shell singlet intermediate. The active site residue Ser219 can stablize the transition state of the dehydration step by a stronger hydrogen bond. The hydrogen bond network formed by the active site residues Glu143, Arg178, and His320 can stablize the protonated His320, which is essential for the catalysis, besides anchoring His320 to the right orientation.

AUTHOR INFORMATION

Corresponding Author

*E-mail: ljy121@jlu.edu.cn.

Notes

The authors declare no competing financial interest.

ACKNOWLEDGMENTS

This work was supported by the National Natural Science Foundation of China (20973077), the Program for New Century Excellent Talents in University (NCET).

REFERENCES

(1) Oinuma, K.-I.; Hashimoto, Y.; Konishi, K.; Goda, M.; Noguchi, T.; Higashibata, H.; Kobayashi, M. *J. Biol. Chem.* **2003**, *278*, 29600−29608.
(2) Xie, S.-X.; Kato, Y.; Komeda, H.; Yoshida, S.; Asano, Y. *Biochemistry* **2003**, *42*, 12056−12066.
(3) Kato, Y.; Yoshida, S.; Xie, S.-X.; Asano, Y. *J. Biosci. Bioeng.* **2004**, *97*, 250−259.
(4) Kato, Y.; Asano, Y. *Appl. Microbiol. Biotechnol.* **2005**, *70*, 92−101.
(5) Oinuma, K.-I.; Ohta, T.; Konishi, K.; Hashimoto, Y.; Higashibata, H.; Kitagawa, T.; Kobayashi, M. *FEBS Lett.* **2004**, *568*, 44−48.
(6) Konishi, K.; Ishida, K.; Oinuma, K.-I.; Ohta, T.; Hashimoto, Y.; Higashibata, H.; Kitagawa, T.; Kobayashi, M. *J. Biol. Chem.* **2004**, *279*, 47619−47625.
(7) Oinuma, K.-I.; Kumita, H.; Ohta, T.; Konishi, K.; Hashimoto, Y.; Higashibata, H.; Kitagawa, T.; Shiro, Y.; Kobayashi, M. *FEBS Lett.* **2005**, *579*, 1394−1398.
(8) Konishi, K.; Ohta, T.; Oinuma, K.-I.; Hashimoto, Y.; Kitagawa, T.; Kobayashi, M. *Proc. Natl. Acad. Sci. U.S.A.* **2006**, *103*, 564−568.
(9) DeMaster, E. G.; Shirota, F. N.; Nagasawa, H. T. *J. Org. Chem.* **1992**, *57*, 5074−5075.
(10) Boucher, J.; Delaforge, M.; Mansuy, D. *Biochemistry* **1994**, *33*, 7811−7818.
(11) Hart-Davis, J.; Battioni, P.; Boucher, J.; Mansuy, D. *J. Am. Chem. Soc.* **1998**, *120*, 12524−12530.
(12) Sawai, H.; Sugimoto, H.; Kato, Y.; Asano, Y.; Shiro, Y.; Aono, S. *J. Biol. Chem.* **2009**, *284*, 32089−32096.
(13) Warshel, A.; Levitt, M. *J. Mol. Biol.* **1976**, *103*, 227−249.
(14) Field, M. J.; Bash, P. A.; Karplus, M. *J. Comput. Chem.* **1990**, *11*, 700−733.
(15) MacKerell.; et al. *J. Phys. Chem. B* **1998**, *102*, 3586−3616.
(16) Brooks, B. R.; et al. *J. Comput. Chem.* **2009**, *30*, 1545−1614.
(17) Brooks, C. L., III; Karplus, M. *J. Chem. Phys.* **1983**, *79*, 6312−6325.
(18) Brooks, C. L., III; Karplus, M. *J. Mol. Biol.* **1989**, *208*, 159−181.
(19) Bakowies, D.; Thiel, W. *J. Phys. Chem.* **1996**, *100*, 10580−10594.
(20) de Vries, A. H.; Sherwood, P.; Collins, S. J.; Rigby, A. M.; Rigutto, M.; Kramer, G. J. *J. Phys. Chem. B* **1999**, *103*, 6133−6141.
(21) TURBOMOLE V6.3 2011, a development of the University of Karlsruhe and Forschungszentrum Karlsruhe GmbH, 1989−2007, TURBOMOLE GmbH, since 2007; available from http://www.turbomole.com.
(22) Sherwood, P.; et al. *J. Mol. Struct. (THEOCHEM)* **2003**, *632*, 1−28.
(23) ChemShell, a Computational Chemistry Shell, see www.chemshell.org.
(24) Smith, W.; Forester, T. *J. Mol. Graph.* **1996**, *14*, 136−141.
(25) Käestner, J.; Carr, J. M.; Keal, T. W.; Thiel, W.; Wander, A.; Sherwood, P. *J. Phys. Chem. A* **2009**, *113*, 11856−11865.
(26) Billeter, S. R.; Turner, A. J.; Thiel, W. *Phys. Chem. Chem. Phys.* **2000**, *2*, 2177−2186.
(27) Henkelman, G.; Uberuaga, B. P.; Jonsson, H. *J. Chem. Phys.* **2000**, *113*, 9901−9904.
(28) Käestner, J.; Sherwood, P. *J. Chem. Phys.* **2008**, *128*, 014106.
(29) Chen, H.; Ikeda-Saito, M.; Shaik, S. *J. Am. Chem. Soc.* **2008**, *130*, 14778−14790.
(30) Wang, D.; Thiel, W. *J. Mol. Struct. (THEOCHEM)* **2009**, *898*, 90−96.